

Measuring the tangle of three-qubit states

Adrián Pérez-Salinas,^{1,2} Diego García-Martín,^{1,2,3} Carlos Bravo-Prieto,^{1,2} and José I. Latorre^{1,4,5}

¹*Departament de Física Quàntica i Astrofísica and Institut de Ciències del Cosmos (ICCUB),
Universitat de Barcelona, Martí i Franquès 1, 08028 Barcelona, Spain.*

²*Barcelona Supercomputing Center, Barcelona, Spain.*

³*Instituto de Física Terica, UAM-CSIC, Madrid, Spain.*

⁴*Center for Quantum Technologies, National University of Singapore, Singapore.*

⁵*Technology Innovation Institute, Abu Dhabi, UAE.*

We present a quantum circuit that transforms an unknown three-qubit state into its canonical form, up to relative phases, given many copies of the original state. The circuit is made of three single-qubit parametrized quantum gates, and the optimal values for the parameters are learned in a variational fashion. Once this transformation is achieved, direct measurement of outcome probabilities in the computational basis provides an estimate of the tangle, which quantifies genuine tripartite entanglement. We perform simulations on a set of random states under different noise conditions to assess the validity of the method.

I. INTRODUCTION

The description of entanglement in a three-qubit system uncovers the subtle and vast problem of classifying and quantifying multipartite entanglement in a reliable way. Although the concept of entanglement is of central importance in the fields of Quantum Information and Computation [1], or in Condensed Matter Physics [2], there is no known general theory of entanglement yet. As the number of qubits increases, an exponentially large number of entanglement invariants under local unitaries can be constructed. Furthermore, the possibility of measuring these entanglement quantifiers on actual states seems out of reach for more than a few qubits [3].

The mainstream approach to deal with multipartite entanglement consists of considering different bipartitions of the system of n qubits and analyze the entanglement that characterizes them. The mathematical tool usually employed is the Singular Value Decomposition, which describes a pure state as a linear combination of product states from the two partitions of the complete system [4]. In turn, the eigenvalues of this decomposition can be used to compute entanglement entropies [5, 6], which are employed to quantify entanglement. For condensed matter systems, the analysis of subsystems of increasing size displays the phenomenon of scaling of the entanglement entropy, often obeying the so-called area law [7].

In contradistinction to bipartite states, there is no simple equivalent to the Singular Value Decomposition for tripartite systems [8, 9]. In that case, the best canonical representation achievable allows to set several coefficients of the original state to zero and fix some of its relative phases through local unitaries. In particular, the canonical form of three-qubit states was found by Acín *et al.* in Ref. [10].

When dealing with pure bipartite states, a variational quantum algorithm [11, 12] can be trained on several copies of the original state in order to discover the local unitaries that reveal its Schmidt form. Then, direct mea-

surements in the computational basis provide the eigenvalues of the Singular Value Decomposition, which in turn are used to compute entanglement entropies. Here, we shall explore a similar strategy to obtain the canonical form and measure the tangle of three-qubit states. We propose a quantum circuit made of three local unitaries, each acting on one of the qubits. The action of these unitaries cast the state into its canonical form, up to relative phases, and can be determined in a variational way. Once this transformation is achieved, the frequencies of measurement outputs in the computational basis are used to compute the tangle of the three-qubit system, which quantifies genuine tripartite entanglement.

The standard procedure for measuring the tangle of a given quantum state involves performing quantum tomography. Such method requires knowledge of 4^3 observables, obtained through 3^3 different measurement settings. In contrast, the algorithm herein proposed only needs one measurement setting, namely measuring in the computational basis, but several copies of the state are demanded for the optimization. Overall, both methods involve a similar number of copies. However, our proposal also returns the canonical form of the state.

The rest of the paper is organized as follows. The tangle of three-qubit states is briefly reviewed in Sec. II. Then, the algorithm for measuring the tangle on a quantum computer is presented in Sec. III. The results of simulations under different noise conditions are shown in Sec. IV. Finally, conclusions are drawn in Sec. V.

II. TANGLE IN THREE-QUBIT STATES

Let us focus now in more detail in tripartite entanglement [13]. Consider a three-qubit system with three partitions, namely, A , B and C ,

$$|\psi\rangle_{ABC} = \sum_{i,j,k=0}^1 t_{ijk} |ijk\rangle, \quad (1)$$

where $\{|ijk\rangle\}$ are the computational-basis states, and the complex coefficients in the tensor t_{ijk} obey a normalization relation. A genuine entanglement measure of a three-qubit system $|\psi\rangle_{ABC}$ is the tangle [14], denoted by τ_{ABC} . It can be obtained from Cayley's hyperdeterminant, which is a generalization of a square-matrix determinant [15]. To be precise,

$$\tau = 4 |\text{Hdet}(t_{ijk})|. \quad (2)$$

In this case, the hyperdeterminant $\text{Hdet}(t_{ijk})$ is a polynomial of order four in the amplitudes t_{ijk} [16],

$$\begin{aligned} \text{Hdet}(t_{ijk}) = & t_{000}^2 t_{111}^2 + t_{001}^2 t_{110}^2 + t_{010}^2 t_{101}^2 + t_{100}^2 t_{011}^2 \\ & - 2(t_{000} t_{111} t_{011} t_{100} + t_{000} t_{111} t_{101} t_{010} + t_{000} t_{111} t_{110} t_{001} + \\ & + t_{011} t_{100} t_{010} t_{010} + t_{011} t_{100} t_{110} t_{001} + t_{101} t_{010} t_{110} t_{001}) \\ & + 4(t_{000} t_{110} t_{010} t_{011} + t_{111} t_{001} t_{010} t_{100}). \end{aligned} \quad (3)$$

The distribution of the tangle τ_{ABC} for three-qubit random states is depicted in Fig. 1. We consider random states with $t_{ijk} = a_{ijk} + i b_{ijk}$ such that a_{ijk} and b_{ijk} are random real numbers between -0.5 and 0.5, further subject to global normalization. These states tend to populate values of the tangle around ~ 0.3 . In contrast, the bipartite Von Neumann entropy of random states tends to be maximum [17].

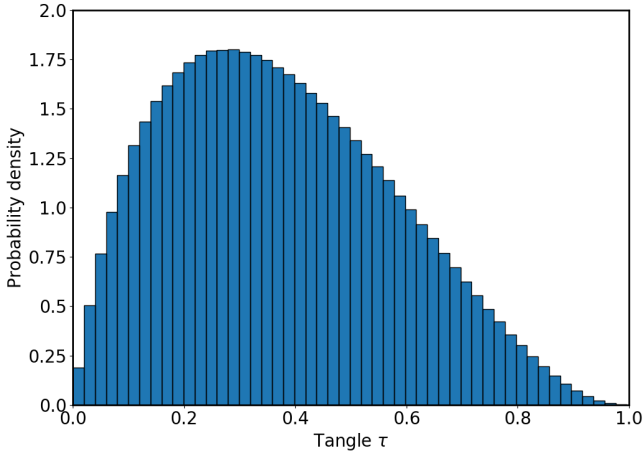


Figure 1. Probability density of random states as a function of the tangle. As can be seen, random states do not have a high tangle, instead they tend to populate values around ~ 0.3 .

In the case of bipartite entanglement, knowledge of the Schmidt coefficients suffices to compute entanglement measures, whereas a full description of a three-qubit state is needed for computing the tangle. However, that being the case, a canonical representation of the three-qubit state may be achieved via local unitary operations (LU), allowing for an easier characterization of the entanglement structure. Note that entanglement is not affected by LU [18]. This property of entanglement invariance

under local unitary operations is a cornerstone of entanglement theory.

In this sense, the canonical representation allows to set several amplitudes of the original state to zero and fix some of its relative phases. A canonical form of a tripartite state such that it respects all its entanglement invariants must be constructed with the use of three local unitaries $U_A \otimes U_B \otimes U_C$, each acting on a partition. For a three-qubit state, the complete rationale for this construction goes as follows. The total number of degrees of freedom of a three-qubit state is 2×2^3 real numbers for the coefficients t_{ijk} , minus a global phase and norm constraints, which makes a total amount of 14. Now, we remove the freedom carried by the three single-qubit unitaries, which is 3×3 . Thus, the number of degrees of freedom is 5. In consequence, there are 5 entanglement invariants under local unitaries [10]. Note that a similar argument applied to n qubits shows that the number of entanglement invariants grows as $2 \times 2^n - 3n - 2$.

It is then always possible to bring a three-qubit state to a canonical form, where three amplitudes are set to zero and only one relative phase remains [10]. This canonical form reads

$$|\varphi\rangle = \lambda_0|000\rangle + \lambda_1 e^{i\phi}|100\rangle + \lambda_2|101\rangle + \lambda_3|110\rangle + \lambda_4|111\rangle, \quad (4)$$

where $\{\lambda_i\}$ are real positive values and ϕ is a relative phase $0 \leq \phi \leq \pi$, attached by convention to $|100\rangle$. Once the canonical form of the tripartite state is obtained, it is possible to compute the 5 entanglement invariants [19] as

$$\begin{aligned} \frac{1}{2} \leq I_1 \equiv \text{Tr} \rho_A^2 &= 1 - 2\mu_0(1 - \mu_0 - \mu_1) \leq 1 \\ \frac{1}{2} \leq I_2 \equiv \text{Tr} \rho_B^2 &= 1 - 2\mu_0(1 - \mu_0 - \mu_1 - \mu_2) - 2\Delta \leq 1 \\ \frac{1}{2} \leq I_3 \equiv \text{Tr} \rho_C^2 &= 1 - 2\mu_0(1 - \mu_0 - \mu_1 - \mu_3) - 2\Delta \leq 1 \\ \frac{1}{4} \leq I_4 \equiv \text{Tr}(\rho_A \otimes \rho_B \rho_{AB}) &= \\ & 1 + \mu_0(\mu_2\mu_3 - \mu_1\mu_4 - 2\mu_2 - 3\mu_3 - 3\mu_4) \\ & - (2 - \mu_0)\Delta \leq 1 \\ 0 \leq I_5 \equiv |\text{Hdet}(t_{ijk})|^2 &= \mu_0^2 \mu_4^2 \leq \frac{1}{16}, \end{aligned} \quad (5)$$

where $\mu_i = \lambda_i^2$ and $\Delta = |\lambda_1 \lambda_4 e^{i\phi} - \lambda_2 \lambda_3|^2$. Therefore, from Eq. (2) and Eq. (5) follows that

$$\tau = 4 \sqrt{I_5} = 4 \mu_0 \mu_4. \quad (6)$$

Consequently, given a state in its canonical form, the tangle can be directly computed as the product of the outcome probabilities of the states $|000\rangle$ and $|111\rangle$ in the computational basis, multiplied by four.

III. QUANTUM ALGORITHM FOR MEASURING THE TANGLE

Let us assume that we receive an unknown three-qubit state $|\psi\rangle$. Our goal is to perform local unitary operations on this state in order to transform it to its canonical form

in Eq. (4). Such operations are defined as

$$|\varphi\rangle = U_A(\vec{\theta}_A) \otimes U_B(\vec{\theta}_B) \otimes U_C(\vec{\theta}_C) |\psi\rangle, \quad (7)$$

where each unitary takes the form

$$U(\vec{\theta}) = \begin{pmatrix} \cos \theta_0/2 & -e^{i\theta_1} \sin \theta_0/2 \\ e^{i\theta_2} \sin \theta_0/2 & e^{i(\theta_1+\theta_2)} \cos \theta_0/2 \end{pmatrix}, \quad (8)$$

with $\vec{\theta} = (\theta_0, \theta_1, \theta_2)$, and $|\varphi\rangle$ is the canonical form of $|\psi\rangle$. It is then necessary to find the values $(\vec{\theta}_A, \vec{\theta}_B, \vec{\theta}_C)_{\text{opt}}$ that achieve this transformation. We will follow a hybrid variational strategy and define

$$(\vec{\theta}_A, \vec{\theta}_B, \vec{\theta}_C)_{\text{opt}} = \text{argmin} \left(\mathcal{C}(\vec{\theta}_A, \vec{\theta}_B, \vec{\theta}_C) \right), \quad (9)$$

where \mathcal{C} is the cost function defined as

$$\begin{aligned} \mathcal{C}(\vec{\theta}_A, \vec{\theta}_B, \vec{\theta}_C) = & \left(|\langle 001|U(\vec{\theta}_A, \vec{\theta}_B, \vec{\theta}_C)|\psi\rangle|^2 + \right. \\ & |\langle 010|U(\vec{\theta}_A, \vec{\theta}_B, \vec{\theta}_C)|\psi\rangle|^2 + \\ & \left. |\langle 011|U(\vec{\theta}_A, \vec{\theta}_B, \vec{\theta}_C)|\psi\rangle|^2 \right). \end{aligned} \quad (10)$$

Notice that the optimal solution, *i.e.*, the configuration $(\vec{\theta}_A, \vec{\theta}_B, \vec{\theta}_C)_{\text{opt}}$ that sets this cost function to 0, transforms $|\psi\rangle$ into an up-to-phases canonical form $|\tilde{\varphi}\rangle$ given by

$$|\tilde{\varphi}\rangle = \lambda_0|000\rangle + \lambda_1 e^{i\phi_1}|100\rangle + \lambda_2 e^{i\phi_2}|101\rangle + \lambda_3 e^{i\phi_3}|110\rangle + \lambda_4 e^{i\phi_4}|111\rangle. \quad (11)$$

Such transformation is less restrictive than the canonical transformation in Eq. (7). Therefore, there exist many possible optimal parameters. The quantum circuit implementing this operation is depicted in Fig. 2.

Once the optimal parameters are obtained, it is straightforward to measure the tangle τ in an actual quantum computer. This quantity will be equal to

$$\tau = 4 |\langle 000|\tilde{\varphi}\rangle \langle 111|\tilde{\varphi}\rangle|^2 = 4 P_{000} P_{111}, \quad (12)$$

where P_{ijk} is the probability of measuring $|ijk\rangle$. The statistical error of P_{ijk} is given by the sampling process of a multinomial distribution, that is $\sqrt{P_{ijk}(1 - P_{ijk})/M}$, where M is the number of measurements.

There is a manner to mitigate random errors occurring when computing the tangle via post-selection. After the optimization is completed, and a low value of the cost function is obtained, it is licit to assume that $|\psi\rangle$ has been properly transformed into $|\tilde{\varphi}\rangle$. Thus, if the outcome of a measurement is either $|001\rangle$, $|010\rangle$ or $|011\rangle$ is due to an error in the circuit. In this case, this outcome can be discarded.

IV. SIMULATIONS

The algorithm for measuring the tangle can be benchmarked on simulations. We have considered a set of 1000

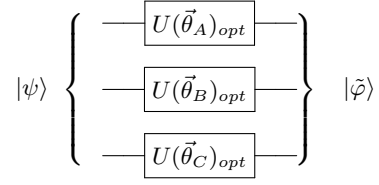


Figure 2. Quantum circuit required for driving an unknown state $|\psi\rangle$ into its up-to-phases canonical form $|\tilde{\varphi}\rangle$. The optimal parameters $(\vec{\theta}_A, \vec{\theta}_B, \vec{\theta}_C)_{\text{opt}}$ are chosen variationally.

random states, accounting for finite sampling and noise. The state $|\text{GHZ}\rangle = (|000\rangle + |111\rangle)/\sqrt{2}$ has been treated as a particular case, as it is the one that maximizes the tangle and, in addition, it is already in its canonical form. To be precise, we sampled 10^4 times and introduced random Pauli errors in the quantum circuits in every run, for increasing noise levels. Each measure of the tangle has been repeated ten times, with and without post-selection. We employed the standard Python Library `Scipy` [20] for the optimization procedure. In particular, we employed the Powell method as it was found to provide accurate results [21]. The mean number of optimization steps is of the order of a few hundred.

Not all optimization instances were found to be satisfactory. Some trials did not reach a proper minimum during the first attempt. In order to avoid outliers, only those instances whose cost function was under a certain threshold were accepted. For those that did not match this criterium, the algorithm was rerun. A maximum number of five attempts were allowed.

A. Error model

We now present the error model that we have used in the simulations. In this model, single-qubit gates can appear randomly with certain probabilities, to be discussed later. These gates modify the state within the quantum circuit and may appear only after applying the unitary gates from Eq. (7). As the algorithm for measuring the tangle does not require the use of entangling gates, we assume that the qubits have no cross-talk, and thus two-qubit errors are omitted.

We consider two different types of error. First, random bit-flips, phase-flips and bit-phase-flips are modeled with Pauli- X , Z , and Y gates respectively. All of them may appear sequentially for each one of the qubits. The second kind of error is measurement errors, which are modeled with a Pauli- X gate appearing just before read-out. A scheme for the occurrence of these gates is shown in Fig. 3.

Every gate has an independent probability of appearing in the circuit, *i.e.*, all error events are uncorrelated.

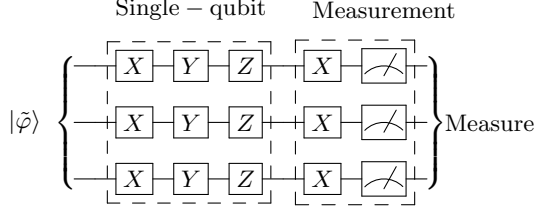


Figure 3. Error model for the simulations. Single-qubit and measurements errors can occur following the scheme of the figure, and may happen with probabilities $0.1t\%$ and $1t\%$, respectively, for $t = \{0, 1, 2, 3, 4, 5\}$. All errors are uncorrelated. This circuit is to be applied after that in Fig. 2.

Therefore, the probability of one error ε occurring is

$$\text{Prob}_\varepsilon = p_\varepsilon \prod_{e \neq \varepsilon} (1 - p_e), \quad (13)$$

where p_e is the probability that one error occurs, and the product runs over all possible errors. This can be easily extended to calculate the probability of occurrence of a higher number of errors.

The probabilities of single-qubit and measurement errors are taken as $0.1t\%$ and $1t\%$ respectively, where $t = \{0, 1, 2, 3, 4, 5\}$ is a tuning parameter. These numbers were selected in agreement with the orders of magnitude present in the experiment in Ref. [22]. Considering $t = 5$, there is one error in $\sim 17\%$ of the samples, and there are $\sim 1.5\%$ of events with two errors. Three or more errors are unlikely to happen, with appearance rates under 0.1% .

As Pauli- X, Y, Z gates do not commute, choosing to apply first one or another is not equivalent. However, the probability of this kind of events is very low. For instance, the probability of two measurement errors is $p \sim 10^{-4}$, of one measurement and one single-qubit error is $p \sim 10^{-5}$, and for two single-qubit errors is only $p \sim 10^{-6}$. Therefore, we choose one particular ordering. Notice as well that the tangle is not affected by some of these errors, such as Pauli- Z errors alone.

B. Results

Two different types of simulations have been carried out. First, we study the $|\text{GHZ}\rangle$ state, which maximizes the tangle, $\tau = 1$. This state is already in its canonical form. Therefore, there is no need for applying single-qubit gates, and no optimization procedure is needed in this case. The averaged results for the tangle obtained without optimization are represented by solid lines in Fig. 4, while the shadowed regions span all results. On the other hand, the full procedure can be applied to the $|\text{GHZ}\rangle$ state as if it were an unknown input state. The results obtained in the latter manner are shown as dots

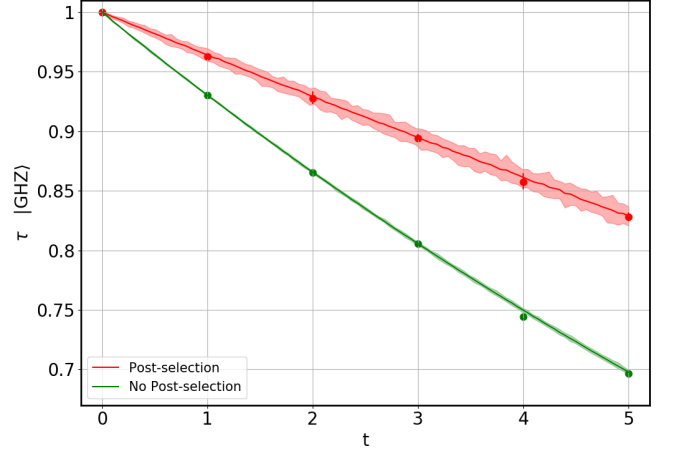


Figure 4. Tangle of the $|\text{GHZ}\rangle$ state vs. parameter t quantifying gate errors. Solid lines represent averaged results for the tangle obtained without optimization, while the shadowed regions span all results. The dots are the results for the full optimization method applied to the $|\text{GHZ}\rangle$ state as if it were an unknown input state. Colors indicate whether post-selection has been applied or not. As we can observe, the optimization procedure does not play a significant role.

in Fig. 4. This allows us to check that the distortion induced by the optimization procedure does not play a significant role. Both methods were simulated with and without post-selection.

Secondly, we consider 1000 random states and simulate the proposed algorithm for measuring the tangle. The final results are depicted in Fig. 5. As could be expected, results are better for post-selected cases. Those random states whose optimization returns a value of the cost function \mathcal{C} above a certain threshold have been discarded. This process cleans the points far from the solid line in Fig. 5. From now, we set said threshold to $t2\%$, i.e., for $t = 5$ we allow a minimization error up to 10% .

From the results obtained, it is possible to see that circuits with no error can estimate the tangle properly. In contrast, circuits with errors present a tendency to return values of the tangle which are lower than the exact ones. Besides, the dispersion also increases with the errors.

We present in Fig. 6 results of the relative errors of the tangle, defined by

$$\Delta\tau = \frac{\tau' - \tau}{\tau}, \quad (14)$$

where τ' is obtained through the variational method, and τ is the exact result. It can be seen that the average behavior of this algorithm is to provide a lower tangle than the exact value. The procedure by itself returns a tangle $\sim -30\%$ lower than the target, while post-processing reduces the error to $\sim -17\%$.

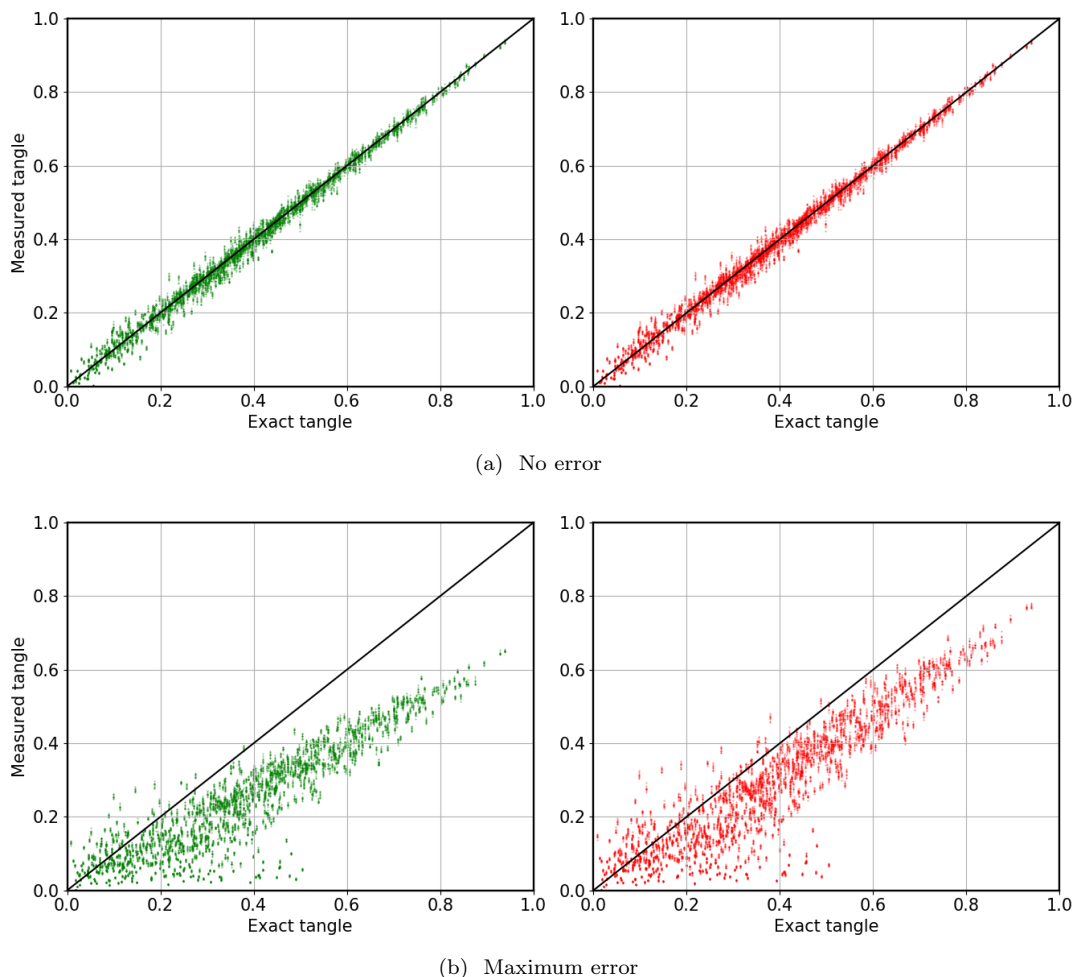


Figure 5. Measured tangle vs. exact tangle, for three-qubit random states. Results in green were obtained without applying post-selection, in contrast to those in red. (a) Results with no gate errors. (b) Results considering the maximum gate error allowed in this paper, $t = 5$. In all figures, the solid black line represents ideal measurement of the tangle. As the errors decrease, we observe convergence towards the exact tangle.

V. CONCLUSIONS

We have presented a variational quantum algorithm that casts an unknown three-qubit state into its canonical form, up to relative phases, given many copies of it. Subsequently, the tangle can be readily measured. The idea behind this procedure is to set three out of eight amplitudes, namely those corresponding to $|001\rangle$, $|010\rangle$ and $|011\rangle$, to zero. Furthermore, a post-selection scheme allows for a mitigation of the errors.

We have performed simulations on a set of random states to benchmark the proposed algorithm under different noise conditions. We have found that the quantum circuit delivers the correct value of the tangle, with a degradation of the results as the noise levels increase. To be precise, assuming errors comparable to those in state-of-the-art quantum processors, the average relative error is of the order of $\sim -17\%$. It is noteworthy that the tangle is, in most cases, underestimated.

This algorithm does not provide an improvement in the required number of copies of the quantum state, compared to quantum tomography. Nevertheless, the method herein proposed also returns the canonical form of the states and, therefore, might be used as a module in other algorithms. For instance, it can be applied as a pre-processing for a quantum classifier. That is, once the canonical form is cast, the quantum classifier may use this feature to distinguish between different quantum states for a particular task.

ACKNOWLEDGEMENTS

APS, DGM, CBP, and JIL are supported by Project PGC2018-095862-B-C22 and acknowledge CaixaBank for its support of this work through Barcelona Supercomputing Center's project CaixaBank Computaci3n Cu3ntica.

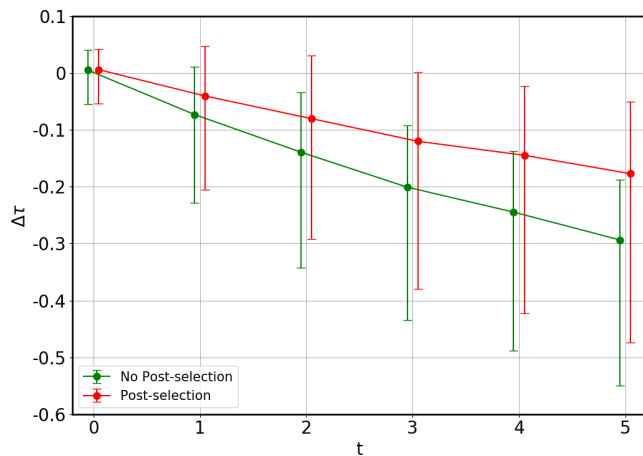


Figure 6. Relative error of the tangle of 1000 random states, with a $2t\%$ threshold in the cost function value, as a function of the error parameter t . Dots correspond to average values, and error bars span 70% of the measurements. Colors indicate whether post-selection has been applied or not. Note that the algorithm measures the correct tangle in the absence of noise, but tends to underestimate the tangle under the presence of it.

-
- [1] M. A. Nielsen and I. L. Chuang, *Quantum Computation and Quantum Information: 10th Anniversary Edition* (Cambridge University Press, 2010).
 - [2] N. Laflorencie, *Physics Reports* **646**, 159 (2016).
 - [3] M. S. Leifer, N. Linden, and A. Winter, *Physical Review A* **69** (2004).
 - [4] A. Ekert and P. L. Knight, *American Journal of Physics* **63**, 415 (1995).
 - [5] J. Neumann, *Mathematical foundations of quantum mechanics* (Princeton University Press Princeton University Press, Princeton, 2018).
 - [6] A. Rényi, in *Proceedings of the Fourth Berkeley Symposium on Mathematical Statistics and Probability, Volume 1: Contributions to the Theory of Statistics* (University of California Press, Berkeley, Calif., 1961) pp. 547–561.
 - [7] J. I. Latorre and A. Riera, *Journal of Physics A: Mathematical and Theoretical* **42**, 504002 (2009).
 - [8] A. Peres, *Physics Letters A* **202**, 1617 (1995).
 - [9] A. K. Pati, *Physics Letters A* **278**, 118 (2000).
 - [10] A. Acín, A. Andrianov, L. Costa, E. Jané, J. I. Latorre, and R. Tarrach, *Phys. Rev. Lett.* **85**, 1560 (2000).
 - [11] R. LaRose, A. Tikku, e. O’Neel-Judy, L. Cincio, and P. J. Coles, *npj Quantum Information* **5** (2019).
 - [12] C. Bravo-Prieto, D. García-Martín, and J. I. Latorre, “Quantum singular value decomposer,” (2019), arXiv:1905.01353 [quant-ph].
 - [13] M. Enríquez, F. Delgado, and K. Zyczkowski, *Entropy* **20**, 745 (2018).
 - [14] V. Coffman, J. Kundu, and W. K. Wootters, *Physical Review A* **61** (2000).
 - [15] A. Cayley, *The collected mathematical papers of Arthur Cayley*, Vol. 1 (The University Press, 1894).
 - [16] I. M. Gelfand, M. M. Kapranov, and A. V. Zelevinsky, *Discriminants, Resultants, and Multidimensional Determinants* (Birkhäuser Boston, 1994).
 - [17] I. Bengtsson and K. Zyczkowski, *Geometry of Quantum States* (Cambridge University Press, 2006).
 - [18] B. Kraus, *Physical Review Letters* **104** (2010).
 - [19] A. Sudbery, *Journal of Physics A: Mathematical and General* **34**, 643652 (2001).
 - [20] P. Virtanen *et al.*, *Nature Methods* (2020).
 - [21] M. J. D. Powell, *The Computer Journal* **7**, 155 (1964).
 - [22] F. Arute *et al.*, *Nature* **574**, 505 (2019).